Fluorescence imaging in pediatric surgery: state-of-the-art and future perspectives.

Paraboschi I[1,2,3], De Coppi P[2,4], Stoyanov, D[1], Anderson J[3,5], Giuliani S[1,4]

1. Wellcome/EPSRC Centre for Interventional & Surgical Sciences, University College London, London, UK.
2. Stem Cells & Regenerative Medicine Section, UCL Great Ormond Street Institute of Child Health, London, UK.
3. Cancer Section, Developmental Biology and Cancer Programme, UCL Great Ormond Street Institute of Child Health, London, UK.
4. Department of Specialist Neonatal and Pediatric Surgery, Great Ormond Street Hospital for Children NHS Foundation Trust, London, UK.
5. Department of Oncology, Great Ormond Street Hospital for Children NHS Foundation Trust, London, England, UK.

Abstract.

The employment of fluorescence imaging has gained popularity in many fields of adult surgery, such as organ perfusion assessment, intra-operative solid tumor identification and sentinel lymph node mapping. In this respect, it has demonstrated great potential to improve both surgical and oncological outcomes while minimizing anesthetic time and lowering health-care costs.

However, the clinical application of Fluorescence-Guided Surgery (FGS) in pediatrics is just at the initial phase. Review of published literature indicates a paucity of clinical studies evaluating FGS in pediatric surgery but huge scope for preclinical investigation and new clinical studies. Great emphasis has been given to the clinical application of FGS for surgical resection of hepatoblastoma and its metastasis and for real-time imaging of the biliary tree. Other current uses of fluorescent imaging in children concern the assessment of blood perfusion and lymphatic flow with the aim to prevent iatrogenic injuries during intestinal and urogenital surgeries. While new and more specific probes are under development, the only fluorescent dyes safely employed in children are currently indocyanine green and fluorescein sodium. Advantages, limitations and potential future development of FGS in pediatrics are systematically discussed and analyzed.

Introduction.

Technological innovations, such as high-resolution Computed Tomography (CT), Magnetic Resonance Imaging (MRI) and Positron Emission Tomography (PET) have brought significant improvements in the pre-operative workup of surgical patients. Nevertheless, their application in the operative room remain challenging as the co-registration of pre-operative images within the surgical field can be difficult and may not always correspond to the definitive intra-operative findings. Moreover, in pediatric surgery, there is an ever increasing need for real-time magnification methods for visualization of tiny anatomical structures and precise delineation of congenital anatomical variants. The recent advent of Fluorescence-Guided Surgery (FGS) has begun to bridge the gap between pre-operative imaging and intraoperative findings. Fluorescent optical imaging has shown great potential to improve surgical outcomes thanks to its ability to distinguish diseased from non-diseased tissues, and possibly reducing iatrogenic injuries (1-3).

Regarding pediatric oncology, FGS has emerged as a promising technique to help surgeons in performing more radical resection (thanks to better visualization of tumor margins) leading to improved survival. Moreover, in case of resection FGS can also assist surgeons in preserving vital structures and organs to improve long-term functional outcomes (1-3). Although most of the current FGS applications are still reported by adult general surgeons, recently there has been an exponential increase in the number of recent publications in pediatric surgery.

Therefore, we performed a systematic review focusing on current clinical applications of FGS in general pediatric surgery while exploring the latest developments and long-term benefits for children.

Methods.

This review was performed according to the Preferred Reporting Items for Systematic Reviews and Metanalysis Statement (http://www.prisma-statement.org/). An extensive search was conducted in the electronic database MEDLINE from inception through January 2020 using various combinations of keywords such as “fluorescent-guided [All Fields]’’ OR ‘‘fluorescence-guided [All Fields]’’ AND “surgery [All Fields]’’. Additional records were identified through hand-searching the references reported in each selected articles. Two researchers (IP and SG) carried out independent data extraction and quality assessment. Any disagreement was resolved by consensus or by arbitration of the other authors not involved in the initial procedure.

The inclusion criteria for the systematic review were original studies, written in English, that reported the clinical use of FGS for the surgical treatment of children (0-18 years old) affected by thoracic, abdominal or urogenital diseases or tumors. Preclinical studies and review papers not reporting own clinical experience were excluded, as well as articles describing neurosurgical, vascular, ophthalmological, ENT, maxillofacial or aesthetic and plastic surgical procedures.

An electronic database (Microsoft Excel 2007, Redmond, WA, USA) was prepared to collect the following information: authors, article title, journal, year of publication, study period, study design, sample size, age at surgery, underlying disease, type of surgical procedure, complications, type of fluorophore selected and imaging system adopted.

Due to the heterogeneity and the small number of studies a meta-analysis of the available data was deemed unfeasible.

Results.

Overview.

As shown in the Prisma flow diagram (Figure 1), 828/846 studies were excluded. 499 were excluded on a title basis, and 220 were excluded on an abstract basis. 127 studies were evaluated on a full-text basis. Out of them, 109 had to be excluded because focused on adult population (n=83), preclinical studies (n=14) or review articles (n=12).

Therefore, 18 studies were included in the systematic review. 8/18 (44.4%) were retrospective studies, 5/18 (27.8%) were case reports, and 3 (16.7%) were case series. There was only a single prospective study investigating the role of fluorescein sodium in suspected Necrotizing EnteroColitis (NEC) cases (4). Finally, Yamada et al. (5) published a review article on ICG imaging for Hepatoblastoma (HB) patients, at the same time describing their extensive institutional experience in detail.

Table 1 summarizes the current clinical applications of FGS in general pediatric surgery: 3 (16.7%) articles focused on real-time imaging of the biliary tree, 3 (16.7%) on viscera perfusion, 3 (16.7%) on lymphatic flow, 6 (33.3%) on radical tumor resection and 2 (11.1%) on urogenital surgery. A single article (5.6%) described a unicentric experience of laparoscopic FGS in children, including 1 cholecystectomy, 2 nephrectomies and 1 varicocelectomy. IndoCyanine Green (ICG) was the dye employed in 17 (94.4%) out of 18 articles and fluorescein sodium in the remaining one.

ICG is a very safe reagent approved by the Food and Drug Administration (FDA) for more than 60 years (6) and since then used in a variety of clinical settings, such as for the evaluation of hepatic function and cardiac output and for retinal angiography (7). Consistent with previous literature, where the incidence of adverse reactions is very low (<0.01%) (8), no adverse events were observed in the pediatrics articles identified in the current review. In particular, no allergic reactions and no alterations in heart rate, blood pressure or respiratory status occurred. Similarly, fluorescein sodium is an inexpensive and safe compound routinely employed in ophthalmological examination. Allergic reactions and hypotension are rare (< 1%) (4) and no side effects occurred.

As shown in Table 1, the fluorescent dyes were administrated following different protocols depending on the authors' choice and clinical indications. For example, for laparoscopic cholecystectomy, Fernandez-Bautista et al (9) stated that just fifteen minutes were required to perfectly visualize the biliary tree after intravenous ICG injection. On the contrary, Esposito et al (10) chose to inject ICG intravenously 18 hours before surgery to selectively accumulate the fluorescent dye mainly in the extrahepatic bile ducts, in this way avoiding any visible fluorescence in the liver parenchyma (Figure 2).

Focusing on Kasai Hepato Porto Enterostomy (HPE), both Yanagi et al (11) and Hirayama et al (12) administered the ICG dye 24 hours before surgery but at two different concentrations: 0.5 mg/kg and 0.1 mg/kg, respectively. Although for viscera perfusion and lymphatic flow imaging, posology, timing and route of administration were

different in each selected study, protocols were more consistent for HB resection. Indeed, for the latter application, most authors applied the standard of 0.5 mg/kg ICG iv injection, 24 to 72 hours prior to surgery.
The fluorescence signal was detected by optical imaging devices marketed by Hamamatsu Photonics in 6 (33.3%) studies, Karl Storz in 5 (27.8%), Stryker in 2 (11.1%), Mizuho Medical Co and Novadaq Technologies in 1 (5.6%) study each. Chen-Yoshioka et al. (13) developed a new optical imaging system (the Medical Imaging Projection System, MIPS) in association with Panasonic AVC Networks Company. 2 (11.1%) authors didn't disclose the imaging system employed.

Current applications divided by anatomical and surgical areas.

3.1 Imaging of the biliary tree

In the last few years, there has been an exponential increase in the number of laparoscopic cholecystectomies performed in children (14, 15). Given the limitation of the abdominal space and the more frequent occurrence of anatomical variations in children, ICG has more recently been employed as a safe fluorescent probe for the intraoperative visualization of the extrahepatic biliary anatomy.
In particular, in 2019, Esposito et al (10) compared the results of 15 ICG to 200 traditional laparoscopic cholecystectomies performed in their center in the last 25 years. As expected, the enhanced mapping of the biliary tree helped to shorten the average operative time (52 vs 69 minutes) and reduce the postoperative complication rate (0 vs 1.9%) in the former group of patients. Similarly, ICG delineated well the biliary anatomy during a laparoscopic cholecystectomy performed in a 13-year-old girl with a long history of recurrent cholelithiasis in the case series on laparoscopic FGS collected by Fernandez-Bautista et al (9).
ICG can be particularly helpful in case of difficult dissection of the proximal biliary tree, such as in Biliary Atresia (BA). Although the HPE procedure has occupied a prominent role by significantly increasing the survival rate in BA, one-third of patients still do not achieve complete clearance of jaundice early after the primary surgery, ultimately requiring transplantation. ICG-FGS was firstly described by Hirayama et al (12) in 2015 as an essential tool for real-time detection of bile exudation from the porta hepatis after dissection of the fibrous tissue during the HPE. The authors suggested that the intraoperative ICG cholangiogram led to better identification of the biliary structures with clear visualization of the fibrous cone. This helped the appropriate level and extent of dissection, therefore resulting in successful surgeries with good long-term clinical outcomes.
Quantitative results were later provided by Yanagi et al (11), who compared the jaundice outcomes of 10 patients undergoing ICG-FCG with 35 historical patients who underwent traditional HPE or hepaticojejunostomy. Despite the small number of patients, all children in the first group postoperatively normalized their bilirubin levels, whereas 12 (34.3%) children in the second group did not (p-value < 0.05). They claimed that this result was

achieved by the enhanced visualization of the hilar micro bile ducts during the surgical dissection.

3.2 Viscera perfusion

During abdominal surgery tissue perfusion can be difficult to evaluate. Traditionally, it has been subjectively evaluated by observing the organ surface color or by assessing the pulsation or the bleeding from the regional arteries. To date, however, some more adjuncts have been employed, such as the application of fluorescent angiography for estimating the blood supply and the intestinal viability during exploratory laparotomy. This can be particularly useful in the field of pediatric surgery in which newborns and children may develop massive intestinal necrosis. In case of severe volvulus or Necrotizing EnteroColitis (NEC) an accurate way for assessing the intestinal vascular supply is crucial to preserve the maximal length of the bowel with the ultimate goal of preventing short bowel syndrome. In this respect, fluorescent angiography may not only provide valuable information on the safest site of resection but it can also help to assess the vascularization of the neo anastomosis.

Numanoglu et al. (4) were the first to report the employment of fluorescein dye during diagnostic laparoscopy of 8 premature infants with suspected NEC. The fluorescein-aided assessment allowed the detection of 3 patients with ischemic bowel segments which were not visible with the naked eye. The dye-enhanced bowel was dissimilar from the ischemic one, which appeared dark under UV light with a yellow filter.

More recently, other authors have reported their experience by using ICG angiography for the intraoperative assessment of intestinal perfusion in children. Iinuma et al. (16) described the case of a 15-year-old boy undergoing a massive necrotic intestinal resection due to a small bowel volvulus. Although ICG angiography had shown an abnormal vascular flow pattern in the distal part of the residual jejunum, improvements in the clinical findings of the intestine supported the surgeons' decision on performing a primary anastomosis. However, a partial stricture developed on the intestinal segment affected by the atypical angiographic findings, which required a surgical revision two weeks later.

Reconstructive intestinal surgeries have also benefited from fluorescent intraoperative perfusion assessment techniques. Being surgical repairs of AnoRectal Malformations (ARM) and Hirschsprung Disease (HD) based on pedicled intestinal grafts and pull-throughs, the real-time assessment of the vascular flow seems to be a promising tool to prevent postoperative strictures and anastomotic leakages. In this respect, Rentea et al. (17) investigated the role of ICG fluorescence angiography to assess rectal and neovaginal pull-throughs in cloacal reconstructions (n=9), complex ARM (n=1) and HD (n=3) repairs. It significantly impacted the intraoperative decision-making process in a third of patients, including the refashioning of an intestinal anastomosis (n=1), choosing a more proximal resection margin (n=2) or completely discharging a portion of bowel (n=1).

Moving beyond, in 2019, Kisaoglu et al (18) described the use of the ICG fluorescence imaging for identifying and managing insufficient graft perfusion in a 4-year-old boy undergoing liver transplantation.

3.3 Lymphatic flow imaging

Fluorescence imaging can also be wisely employed for guiding the surgical treatment of congenital lymphatic malformations and lymphatic ducts injuries (spontaneous or iatrogenic). Shirota et al (7) described the successful resection of a lymphatic malformation of the abdominal wall in a 15-year-old boy by utilizing ICG fluorescence imaging. Shirotsuki et al (19) collected a series of 10 neonates diagnosed with Esophageal Atresia/TracheoEsophageal Fistula (EA/TEF) in whom ICG imaging was performed to detect the thoracic duct (n=8) at the first repair and to identify the chylous leakage points, as postoperative chylothorax after thoracoscopic surgery was noted (n=3). Similarly, fluorescence lymphatic imaging allowed the successful visualization of abnormal lymphatic drainage in a 5-week-old infant who developed a chylothorax after cardiac surgery in the case report reported by Tan et al (20).

3.4 Tumor resection

Real time visualization of active neoplastic cells has obvious potential for refining surgical approaches for pediatric solid tumors. Although ICG navigation imaging for HepatoCellular Carcinoma (HCC) resection was first described in 2009 (21, 22), its application to pediatric HB detection was attempted for the first time only in 2015 (23). In particular, Yamamichi et al (23) ran the first pilot study evaluating the benefits of ICG navigation surgery for identifying small viable HB tumors. A primary HB of the right lobe, a recurrent HB located between the right diaphragm and the cut surface of the previous surgery and bilateral multiple lung metastases were visualized and safely excised in three children aged one, six and two years respectively.

The same year, Kitagawa et al (24) published the resection of 250 fluorescence-positive pulmonary lesions from 10 patients affected by metastatic HBs (mean age: 4 years; range: 4 months – 11 years and 4 months). The visual fluorescence contrast of the metastatic lesions affecting the peripheral areas of the lung along with the intraoperative collapse of the lung allowed by the one-lung ventilation system led to precise metastatic tumor resections.

Moreover, four years later, Takahashi et al (25) described the case of a 14-year-old-boy who successfully underwent metastasectomy of peritoneally disseminated HBs with ICG navigation followed by second Living Donor Liver Transplantation (LDLTx).

Not only a Charge-Coupled Device (CCD) but also other types of cameras have been safely employed for ICG detection during HB surgery in children. For instance, Chen-Yoshioka et al (13) developed the Medical Imaging Projection System (MIPS, Panasonic AVC Networks Company, Osaka, Japan), that was able to detect ICG

fluorescence of lung HB metastases even with the operating lights turned on and to project the image in visible light back onto the organ being operated on.

More recently, Souzaki et al (26) published the largest series of 5 patients undergoing 10 ICG surgeries (n=4 liver resections, n=6 metastasectomies) by using a 10-mm endoscopic ICG NIRF imaging system (D-LIGHT P, Karl Storz, Germany). The telescopic detector had the advantages of keeping the scope tip closer to the tumor and of perfectly darkening the surgical field. All these elements led to an increased surgical accuracy with a better appreciation of the tumor margins and of its spread to the surrounding structures.

Finally, Yamada et al (5) published their unicentric institutional experience, which includes 13 laparotomies for 12 children with primary tumors of the liver, 15 thoracotomies for 7 patients with pulmonary metastases and 5 surgeries for 4 patients with lymph-node metastasis (n = 1), peritoneal metastasis (n = 2), pancreatic metastasis (n = 1) and bone metastasis (n = 1). They also analyzed current literature on this topic, proposing protocols for fluorophore administration, tumor imaging and surgical excision.

In the near future, with the increase of number of cases, real-time navigation surgery by using ICG will likely become the standard procedure for HB resection thanks to its power for accurately identifying tumor margins and extensions. In addition, by replacing the need of tumor palpation, ICG fluorescence will provide invaluable aid to thoracoscopic resections of HB lung metastases, leading to less invasive surgeries.

3.5 Urogenital surgery

The latest literature shows that also pediatric urology has employed fluorescent optical imaging to improve its performance. The visualization of the urinary tract has greatly facilitated both demolitive and reconstructive urogenital surgeries, leading to more precise procedures and fewer complications.

Initially described for segmental arterial mapping during pediatric Robot-Assisted Laparoscopic HemiNephrectomy (RALHN) (27), the intravenous injection of ICG was then also employed to enhance the visualisation of blood and lymphatic vessels during laparoscopic varicocelectomy (9, 28-30).

In particular, ICG-FGS proved to be a valuable tool in reducing the incidence of innocent moiety injury in 6 pediatric RALHNs in the series reported by Herz et al. (27). Real-time delineation of the selective arterial anatomy of both moieties was performed safely without any toxicity or vascular complications. ICG-FGS helped in alerting surgeons about unexpected renal vascular anatomy and possible iatrogenic injuries to the remaining moiety, thus adding invaluable information during surgery.

In addition, ICG optical imaging was also safely employed to accurately study the renal vascular anatomy in two patients undergoing retroperitoneal laparoscopic nephrectomies in the series collected by Fernandez-Bautista et al. (9).

The same authors (9) reported the use of an intravenous injection of ICG to perform an angiography-assisted

laparoscopic varicocelectomy in a 13-year-old boy with asymmetric testes and testicular pain.

Conversely, Esposito et al. (30) described ICG fluorescence lymphography as a new technique to perform lymphatic sparing laparoscopic Palomo varicocelectomy: none of the 25 boys reported in their series developed a postoperative hydrocele.

Discussion.

FGS has more recently been introduced as a promising tool to overcome the limits of traditional surgeries based on conventional imaging. Especially in the field of oncology, FGS has been emerging as a cutting-edge innovation in which very accurate margin definitions led to more radical tumor resections with better functional outcomes (1).

By combining significant tissue contrast, high sensitivity and specificity and by avoiding exposure of children to ionizing radiations, FGS will lead general pediatric surgery toward patient-customized treatments, in which extremely accurate procedures will be performed according to individual patient anatomy and disease process.

Although the past decade has no doubt witnessed significant advances in the clinical application and technical development of fluorescent optical imaging in the field of general pediatric surgery, there is still need for further advancements and more areas of clinical applications.

Development of new fluorescence imaging probes. Current biomedical fluorescence imaging operates in the spectrum of the visible light (400-700 nm) with some extending in the NearInfraRed (NIR, 700-900 nm). The latter, however, have been usually favored since fluorophores emitting light in the color window are more significantly hindered by tissue autofluorescence and absorbance. NIR dyes arise from less absorbance in tissue and are easily detected up to 10 mm deep (1). Amongst them, ICG and fluorescein sodium have been preferred in general pediatric surgery thanks to their high safety index and their good pharmacokinetic profile.

However, further development of imaging devices is underway. In particular, imaging in the ShortWave IR (SWIR; 1,000-2,000 nm) promises high contrast, sensitivity and penetration depths (31). Remarkably, recent spectroscopic characterization of NIR dyes has revealed that they also have non-negligible emission tails in the SWIR window. Repurposing already FDA approved NIR fluorescent probes as SWIR agents may have significant clinical impacts in future.

Designing fluorescent imaging probes with higher target organ selectivity. Improving the ratio of target to background binding through the development of novel molecular imaging probes are currently under investigation to maximize the signal from the target and minimize the background noise. The aim is to improve the probes' sensitivity and specificity to selectively identify structures at risk of iatrogenic injury and to increase the accuracy of tumor margin delineation with minimal background noise.

Smart tumor-targeted probes, like activatable fluorescent probes and receptor-targeted probes, are now emerging in preclinical and clinical studies in adult oncology (1). Activatable fluorescent probes exist in the quenched state until they are activated by enzymatic cleavage either on the cell membrane (the enzyme reactive activatable fluorescent probes) or in the intracellular lysosomes (the molecular-binding activatable fluorescent probes). By being activated and emitting signals only when engaged within the target, activatable fluorescent probes highly enhanced tumor margin detection in preclinical studies (1).

Furthermore, conjugated monoclonal antibodies are a new generation of agents that having specific recognition sites in their structure also led to significant improvements in adult oncology. Although a few of them have already progressed into clinical trials, cetuximab-IRDye800CW and bevacizumab-IRDye800CW have been successfully employed in targeting head and neck, colon and breast cancers and pancreatic adenocarcinomas in patients (1, 2, 32).

A limitation in the introduction of fluorescent optical imaging into the surgical practice has been the fact that the quenching process takes hours even days to occur. New sprayable targeted probes are under development, and they can be applied into the region of interest by a simple spray, making their clinical use very convenient.

Moreover, complementary analytical tools, such as Artificial Intelligence (AI), will be integrated into an FGS system to improve the decision-making capability of fluorescence optical imaging.

Finally, the incorporation of FGS to laparoscopic devices will favorably supplement the tactile-limited field of minimally invasive surgery, extending its clinical applications in children.

Conclusion.

In recent years FGS has brought forth new lights in pediatric surgery by improving the accuracy of anatomical delineation and helping guide tumor resection in children. With further advancement in fluorophores and imaging system design, FGS will develop as an essential navigation tool in pediatric surgery. It will enable surgeons to personalize the procedures in relation to specific congenital anatomical variants and illness behaviors, at the same time reducing the risks of iatrogenic injuries or inadequate tumor resection. Thanks to all these benefits, FGS is likely to soon become standard of care for children requiring surgery.

Acknowledgment.

References.

1. Nagaya T, Nakamura YA, Choyke PL, Kobayashi H. Fluorescence-Guided Surgery. Front Oncol. 2017;7:314.
2. Tipirneni KE, Warram JM, Moore LS, Prince AC, de Boer E, Jani AH, et al. Oncologic Procedures Amenable to Fluorescence-guided Surgery. Ann Surg. 2017;266(1):36-47.
3. Vahrmeijer AL, Hutteman M, van der Vorst JR, van de Velde CJ, Frangioni JV. Image-guided cancer surgery using near-infrared fluorescence. Nat Rev Clin Oncol. 2013;10(9):507-18.
4. Numanoglu A, Millar AJ. Necrotizing enterocolitis: early conventional and fluorescein laparoscopic assessment. J Pediatr Surg. 2011;46(2):348-51.
5. Yamada Y, Ohno M, Fujino A, Kanamori Y, Irie R, Yoshioka T, et al. Fluorescence-Guided Surgery for Hepatoblastoma with Indocyanine Green. Cancers (Basel). 2019;11(8).
6. FOX IJ, BROOKER LG, HESELTINE DW, ESSEX HE, WOOD EH. A tricarbocyanine dye for continuous recording of dilution curves in whole blood independent of variations in blood oxygen saturation. Proc Staff Meet Mayo Clin. 1957;32(18):478-84.
7. Shirota C, Hinoki A, Takahashi M, Tanaka Y, Tainaka T, Sumida W, et al. New Navigation Surgery for Resection of Lymphatic Malformations Using Indocyanine Green Fluorescence Imaging. Am J Case Rep. 2017;18:529-31.
8. Speich R, Saesseli B, Hoffmann U, Neftel KA, Reichen J. Anaphylactoid reactions after indocyanine-green administration. Ann Intern Med. 1988;109(4):345-6.
9. Fernández-Bautista B, Mata DP, Parente A, Pérez-Caballero R, De Agustín JC. First Experience with Fluorescence in Pediatric Laparoscopy. European J Pediatr Surg Rep. 2019;7(1):e43-e6.
10. Esposito C, Corcione F, Settimi A, Farina A, Centonze A, Esposito G, et al. Twenty-Five Year Experience with Laparoscopic Cholecystectomy in the Pediatric Population-From 10 mm Clips to Indocyanine Green Fluorescence Technology: Long-Term Results and Technical Considerations. J Laparoendosc Adv Surg Tech A. 2019;29(9):1185-91.
11. Yanagi Y, Yoshimaru K, Matsuura T, Shibui Y, Kohashi K, Takahashi Y, et al. The outcome of real-time evaluation of biliary flow using near-infrared fluorescence cholangiography with Indocyanine green in biliary atresia surgery. J Pediatr Surg. 2019;54(12):2574-8.
12. Hirayama Y, Iinuma Y, Yokoyama N, Otani T, Masui D, Komatsuzaki N, et al. Near-infrared fluorescence cholangiography with indocyanine green for biliary atresia. Real-time imaging during the Kasai procedure: a pilot study. Pediatr Surg Int. 2015;31(12):1177-82.
13. Chen-Yoshikawa TF, Hatano E, Yoshizawa A, Date H. Clinical application of projection mapping technology for surgical resection of lung metastasis. Interact Cardiovasc Thorac Surg. 2017;25(6):1010-1.
14. Suh SG, Choi YS, Park KW, Lee SE. Pediatric cholecystectomy for symptomatic gallstones unrelated to hematologic disorder. Ann Hepatobiliary Pancreat Surg. 2016;20(4):187-90.
15. Mehta S, Lopez ME, Chumpitazi BP, Mazziotti MV, Brandt ML, Fishman DS. Clinical characteristics and risk factors for symptomatic pediatric gallbladder disease. Pediatrics. 2012;129(1):e82-8.
16. Iinuma Y, Hirayama Y, Yokoyama N, Otani T, Nitta K, Hashidate H, et al. Intraoperative near-infrared indocyanine green fluorescence angiography (NIR-ICG AG) can predict delayed small bowel stricture after ischemic intestinal injury: report of a case. J Pediatr Surg. 2013;48(5):1123-8.
17. Rentea RM, Halleran DR, Ahmad H, Sanchez AV, Gasior AC, McCracken K, et al. Preliminary Use of Indocyanine Green Fluorescence Angiography and Value in Predicting the Vascular Supply of Tissues Needed to Perform Cloacal, Anorectal Malformation, and Hirschsprung Reconstructions. Eur J Pediatr Surg. 2019.

18. Kisaoglu A, Demiryilmaz I, Dandin O, Ozkan O, Aydinli B. Management of reperfusion deficiency with indocyanine green fluorescence imaging during deceased donor liver transplantation in a pediatric recipient. HPB (Oxford). 2019.
19. Shirotsuki R, Uchida H, Tanaka Y, Shirota C, Yokota K, Murase N, et al. Novel thoracoscopic navigation surgery for neonatal chylothorax using indocyanine-green fluorescent lymphography. J Pediatr Surg. 2018;53(6):1246-9.
20. Tan IC, Balaguru D, Rasmussen JC, Guilliod R, Bricker JT, Douglas WI, et al. Investigational lymphatic imaging at the bedside in a pediatric postoperative chylothorax patient. Pediatr Cardiol. 2014;35(7):1295-300.
21. Gotoh K, Yamada T, Ishikawa O, Takahashi H, Eguchi H, Yano M, et al. A novel image-guided surgery of hepatocellular carcinoma by indocyanine green fluorescence imaging navigation. J Surg Oncol. 2009;100(1):75-9.
22. Ishizawa T, Fukushima N, Shibahara J, Masuda K, Tamura S, Aoki T, et al. Real-time identification of liver cancers by using indocyanine green fluorescent imaging. Cancer. 2009;115(11):2491-504.
23. Yamamichi T, Oue T, Yonekura T, Owari M, Nakahata K, Umeda S, et al. Clinical application of indocyanine green (ICG) fluorescent imaging of hepatoblastoma. J Pediatr Surg. 2015;50(5):833-6.
24. Kitagawa N, Shinkai M, Mochizuki K, Usui H, Miyagi H, Nakamura K, et al. Navigation using indocyanine green fluorescence imaging for hepatoblastoma pulmonary metastases surgery. Pediatr Surg Int. 2015;31(4):407-11.
25. Takahashi N, Yamada Y, Hoshino K, Kawaida M, Mori T, Abe K, et al. Living Donor Liver Re-Transplantation for Recurrent Hepatoblastoma in the Liver Graft following Complete Eradication of Peritoneal Metastases under Indocyanine Green Fluorescence Imaging. Cancers (Basel). 2019;11(5).
26. Souzaki R, Kawakubo N, Matsuura T, Yoshimaru K, Koga Y, Takemoto J, et al. Navigation surgery using indocyanine green fluorescent imaging for hepatoblastoma patients. Pediatr Surg Int. 2019;35(5):551-7.
27. Herz D, DaJusta D, Ching C, McLeod D. Segmental arterial mapping during pediatric robot-assisted laparoscopic heminephrectomy: A descriptive series. J Pediatr Urol. 2016;12(4):266.e1-6.
28. Shibata Y, Kurihara S, Arai S, Kato H, Suzuki T, Miyazawa Y, et al. Efficacy of Indocyanine Green Angiography on Microsurgical Subinguinal Varicocelectomy. J Invest Surg. 2017;30(4):247-51.
29. Tomita K, Kageyama S, Hanada E, Yoshida T, Okinaka Y, Kubota S, et al. Indocyanine Green Angiography-assisted Laparoendoscopic Single-site Varicocelectomy. Urology. 2017;106:221-5.
30. Esposito C, Turrà F, Del Conte F, Izzo S, Gargiulo F, Farina A, et al. Indocyanine Green Fluorescence Lymphography: A New Technique to Perform Lymphatic Sparing Laparoscopic Palomo Varicocelectomy in Children. J Laparoendosc Adv Surg Tech A. 2019;29(4):564-7.
31. Carr JA, Franke D, Caram JR, Perkinson CF, Saif M, Askoxylakis V, et al. Shortwave infrared fluorescence imaging with the clinically approved near-infrared dye indocyanine green. Proc Natl Acad Sci U S A. 2018;115(17):4465-70.
32. Rosenthal EL, Warram JM, de Boer E, Chung TK, Korb ML, Brandwein-Gensler M, et al. Safety and Tumor Specificity of Cetuximab-IRDye800 for Surgical Navigation in Head and Neck Cancer. Clin Cancer Res. 2015;21(16):3658-66.

PRISMA 2009 Flow Diagram

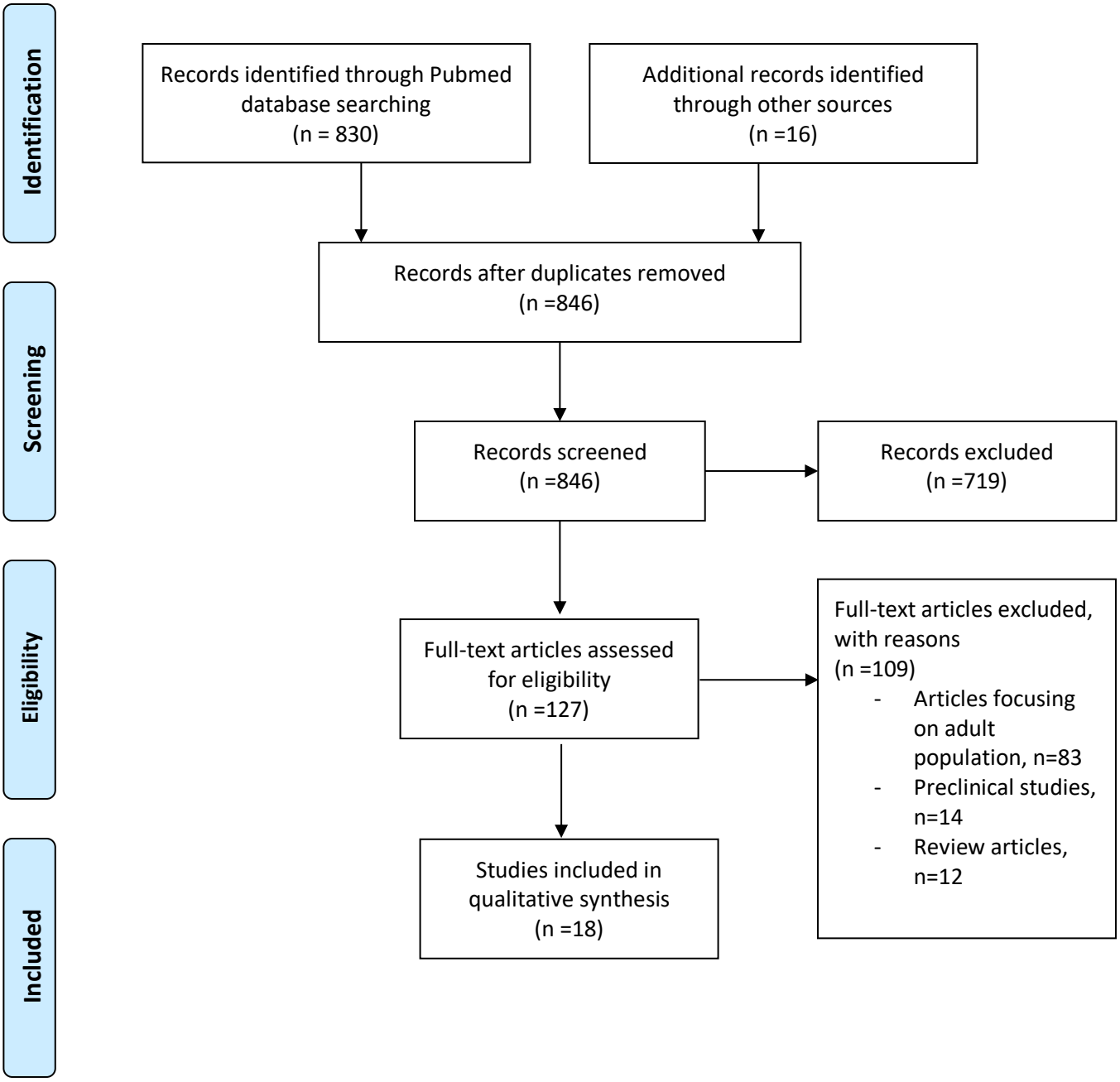

From: Moher D, Liberati A, Tetzlaff J, Altman DG, The PRISMA Group (2009). *P*referred *R*eporting *I*tems for *S*ystematic Reviews and *M*eta-*A*nalyses: The PRISMA Statement. PLoS Med 6(7): e1000097. doi:10.1371/journal.pmed1000097

For more information, visit www.prisma-statement.org.

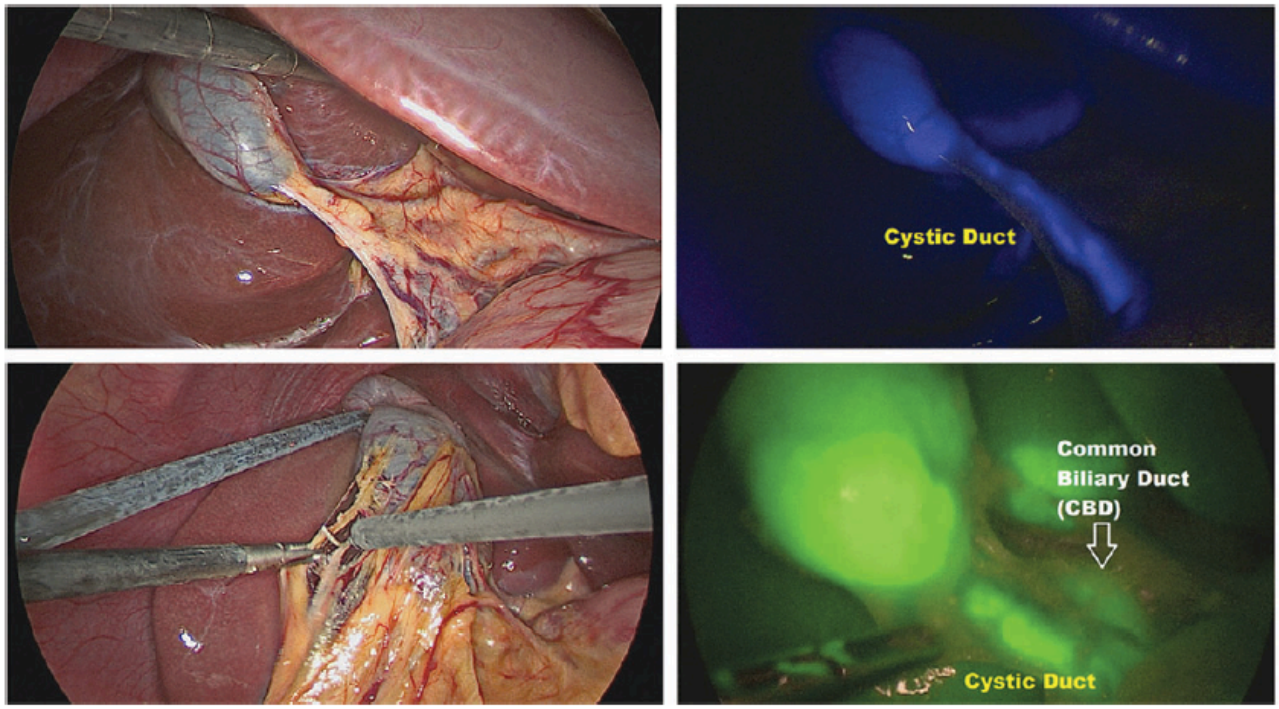

Courtesy of C. Esposito

Figure 2.
ICG fluorescence made identification of the cystic duct easier despite the presence of abundant fatty tissue or adherences.

Author, year	Disease treated (n. of patients affected)	Type of surgery performed (n. of patients per type of procedure)	Study period	Patients' age at surgery	Dye (administration route and dosage)	Imaging system, company
Anatomic imaging of the biliary tree						
Esposito et al, 2019 [10]	Cholelithiasis (n=15)	Laparoscopic cholecystectomy (n=15)	2016-2018	nd	ICG (iv, 0.4 mg/kg, 18 hrs before surgery)	Image1 S™, Karl Storz
Yanagi et al, 2019 [11]	Biliary Atresia (n=10)	Kasai Hepato PortoEnterostomy (n=9); hepaticojejunostomy (n=1)	2017-2018	Median: 69.5 ds (48-122 ds)	ICG (iv, 0.5 mg/kg, 24 hrs before surgery)	Vitom®, Karl Storz
Hirayama et al, 2015 [12]	Biliary Atresia (n=5)	Kasai HepatoPortoEnterostomy (n=5)	2012-2014	Median: 42 ds (31-75 ds)	ICG (iv, 0.1 mg/kg, 24 hrs before surgery)	Photo Dynamic Eye, Hamamatsu Photonics
Viscera perfusion						
Rentea et al, 2019 [17]	Cloaca (n=9), Rectal Atresia (n=1), Hirschsprung Disease (n=3)	Posterior Sagittal AnoRectoVaginoURetroPlasty (PSAVUP) (n=8), Redo PSARVUP (n=1), Colonic pull-through (n=1), Redo pull-through (n=3)	2014-2018	Mean: 1.9 yrs (0.5-7.8 yrs)	ICG (iv, 0.1-0.3 mg/kg, at time of surgery)	SPY Elite Imaging System, Stryker
Iinuma et al, 2013 [16]	Small intestinal volvulus (n=1)	Primary intestinal anastomosis (n=1)	2013	15 yrs	ICG (iv, 25 mg, at time of surgery)	Photo Dynamic Eye, Hamamatsu Photonics
Numanoglu et al, 2011 [4]	Suspected Necrotizing EnteroColitis (n=8)	Diagnostic laparoscopy followed by bowel resection and stoma formation (n=8)	nd	24.5 ds (10-38 ds)	Fluorescein (iv, 14 mg/kg, at time of surgery)	Karl Storz
Lymphatic flow imaging						
Shirotsuki et al, 2018 [19]	Esophageal Atresia/TracheoOesophageal Fistula (n=10)	Diagnostic thoracoscopy (n=8), thoracoscopic ligation of the injured thoracic duct (n=3)	2014-2017	Median: 2.0 ds (1.0-10 ds) Median: 18 ds (13-25 ds)	ICG (iv, 0.025 mg, 1 hr prior to surgery)	Image1 S™, Karl Storz
Shirota et al, 2017 [12]	Lymphatic malformation of the abdominal wall	Surgical resection	2013	15 yrs	ICG (sc and id, 0.125 mg, 20 hrs prior to surgery)	Photo Dynamic Eye (PDE), Hamamatsu Photonics
Tan et al, 2014 [20]	Iatrogenic chylothorax	Diagnostic imaging of the lymphatic flow followed by bilateral pleurodesis	2014	5 wks	ICG (id, 1st injection 25 mcg, 2nd injection 12.5 mcg 19 min later, 3rd injection 12.5 mcg 26 min later)	nd
Tumour resection						
Souzaki et al, 2019 [26]	Primary HB (n=3), HB lung metastases (n=1), primary and HB lung metastases (n=1)	Extended right hepatectomy (n=3), liver transplantation (n=1), lung partial resection (n=5), upper lobectomy (n=1)	2017-2018	Mean: 30.9 mo (12-36 mo)	ICG (iv, 0.5 mg/kg, 60-138 hrs prior to liver surgery, 18-27 hrs prior to lung metastatectomy)	D-LIGHT P, Karl Storz
Takahashi et al, 2019 [25]	HB Peritoneal dissemination (n=1)	Surgical excision (n=1)	nd	14 yrs	ICG (iv, 0.5 mg/kg, 72 hrs prior to surgery)	PhotoDynamic Eye (PDE), Hamamatsu Photonics
Yamada et	Primary HB (n=12), HB	Liver resection (n=13), lung	2014-	Mean: 5.0 yrs	ICG (iv, 0.5	PhotoDyna

al, 2019 [5]	lung metastases (n=7), mediastinal metastasis (n=1), peritoneal metastasis (n=1), pancreatic metastasis (n=1), bone metastasis (n=1)	metastasectomies (n=15), other metastasectomies (n=5)	2019	(0.5-14 yrs)	mg/kg, 72 hrs prior to surgery	mic Eye (PDE), Hamamatsu Photonics
Chen-Yoshioka et al, 2017 [13]	HB lung metastasis (n=1)	Lung metastatectomy (n=1)	nd	3 yrs	ICG (0.5 mg/kg, 24 hrs prior to surgery	Medical Imaging Projection System, Panasonic AVC Networks Company
Kitagawa et al, 2015 [24]	HB lung metastases (n=10)	Lung metastatectomies (n=37)	2012-2014	Mean: 3.5 yrs (1-11 yrs)	ICG (iv, 0.5 mg/kg, 24 hrs prior to surgery)	PhotoDynamic Eye, Hamamatsu Photonics
Yamamichi et al, 2015 [23]	Primary HB (n=1), recurrent HB (n=1), HB lung metastasis (n=1)	Right hepatectomy (n=1), residual tumour and diaphragm resection (n=1), lung metastasectomy (n=1)	nd	Mean: 3 yrs (1-6 yrs)	ICG (iv, 0.5 mg/kg, 72-96 hrs prior to surgery)	HyperEye Medical System, Mizuho Medical Co
Urogenital surgery						
Esposito et al, 2019 [30]	Varicocele (n=25)	Laparoscopic Palomo varicocelectomy (n=25)	2017-2018	Mean: 13.7 yrs (12-16 yrs)	ICG (intratesticular, 0.1 mg, at time of surgery)	nd
Herz et al, 2016 [27]	Duplex kidney (n=6)	Robot-assisted laparoscopic heminephrectomy (n=6)	2014-2016	Mean: 5.6 yrs (0.8-13.2 yrs)	ICG (iv, 1.25-2.5 mg, 30-60 s prior to surgery)	Firefly, da Vinci, Novadaq Technologies Inc
Articles reporting multiple surgical diseases treated with FGS						
Fernàndez-Bautisra et al, 2019 [9]	Cholelithiasis (n=1); varicocele (n=1); renal failure (n=2)	Laparoscopic cholecystectomy (n=1); laparoscopic Palomo varicocelectomy (n=1); laparoscopic nephrectomy (n=2)	nd	Mean: 8.6 yrs (3-13 yrs)	ICG (iv, nd, 15 min before laparoscopic cholecystectomy; iv, nd, at the time of laparoscopic Palomo varicocelectomy; iv, 0.2 mg/kg, at time of laparoscopic nephrectomy)	1488 HD 3-Chip camera system, Stryker

Table 1.
Current literature focusing on Fluorescence-Guided Surgery (FGS) in general paediatric surgery.

Abr. ICG: Indocyanine green; HB: HepatoBlastoma; iv: intravenously; sc: subcutaneously; id: intradermal; yrs: years; mo: months; ds: days; hrs: hours; min: minutes; s: seconds